C.P. No. 136

Technical Note No. Aero 2184

August, 1952

ROYAL AIRCRAFT ESTABLISHMENT

Curves for Estimating the Wave Drag of some Bodies of Revolution, Based on Exact and Approximate Theories

by

L. E. Fraenkel

SUMMARY

Curves are presented for estimating the wave drag, at zero incidence, of forebodies and afterbodies having straight and parabolic profiles. The afterbodies are assumed to lie behind an infinitely long cylindrical body. The curves are based on a limited number of exact and second-order solutions which have been generalised by appealing to the supersonic-hypersonic similarity law and to slender body and quasi-cylinder solutions.

LIST OF CONTENTS

		Page
1	Introduction	3
2	The basis of the generalised curves	4
	2.1 Conical forebodies	4
	2.2 Parabolic forebodies	5
	2.3 Conical afterbodies	5
	2.4 Parabolic afterbodies	5
3	Conclusions	5
References		6
		7

LIST OF ILLUSTRATIONS

	Fig.
Exact and approximate results for cones	1
Exact and approximate results for pointed parabolic (or ogival) forebodies	2
Second-order and approximate results for conical afterbodies	3
Exact and approximate results for parabolic afterbodies	4
Supersonic wave drag of conical forebodies	5
Supersonic wave drag of parabolic forebodies	6
Supersonic wave drag of conical afterbodies	7
Supersonic wave drag of parabolic afterbodies	8

1 Introduction

In Ref. 1 the quasi-cylinder and slender body theories[2,3] were used to establish a reversibility theorem and to introduce the concept of the interference effect of a forebody on an afterbody. For a body consisting of a forebody, a cylindrical mid-portion, and an afterbody, the drag was considered to be the sum of three components:*

(i) The forebody drag.

(ii) The principal afterbody drag, which is the drag that the afterbody could have if it were situated behind an infinitely long parallel portion.

(iii) The interference drag due to the effect of the forebody on the afterbody.

The forebody drag and principal afterbody drag were equal for shapes which are the reverse of one another, and the interference drag proved to be merely the integral over the afterbody of the pressures which would exist on the parallel portion if it were extended into the region of the afterbody.

These concepts and both the approximate theories were then applied to calculate the drag of bodies with pointed or truncated forebodies and afterbodies, of straight or parabolic profile. However the resulting curves are not wholly satisfactory from the viewpoint of the aircraft designer because they are limited to bodies of small profile slope and to fairly low supersonic Mach numbers, and in regions where the approximations begin to differ the designer must decide which of the two theories is nearer to the truth.

This note is an attempt to provide curves of forebody drag and principal afterbody drag which can be used for bodies of moderate profile slope and for fairly high supersonic Mach numbers, and which eliminate the need for choosing one of the two approximations. (No new values of interference drag are provided because no systematic exact solutions of this problem have become available; however, this drag is often small and the approximate values of Ref. 1 may prove adequate for most purposes). The new curves are essentially based on a limited number of exact and second-order results which have been generalised by plotting them according to the supersonic-hypersonic similarity law[4,5] and by extending them on the basis of comparison with the quasi-cylinder and slender body theories. The similarity law can be stated in a number of equivalent ways: the one considered most convenient and used here is that, for bodies of similar profile and different thickness ratios (R/ℓ), the parameter $C_D\,(\ell/R)^2$ is a function only of $R\sqrt{M^2-1}/\ell$. The mathematical derivation of this law rests on an assumption of small profile slope for both the supersonic and hypersonic cases, but checks of the law with exact numerical results (Ref. 6 and the work below) indicate that if the drag of bodies with maximum slopes up to 0.4 is plotted according to the law the maximum deviation from a mean curve is about 5%.

---

* It is assumed both in Ref. 1 and here that the flow is undisturbed ahead of an open-nose body, i.e. that there is no 'spillage'.

All the results given here tend to fail as $M \to 1$; a possible criterion for their applicability is that the flow must be supersonic everywhere in the field ahead of the base. This can generally be investigated by using oblique or cone shock tables to see whether the nose shock is attached and the flow behind it supersonic.

No attempt is made here to allow for the effects of boundary layers, which are known to have a considerable effect on the pressure distribution of afterbodies.

2 The basis of the generalised curves

2.1 Conical forebodies

Fig. 1 shows a comparison on the basis of the similarity law of exact[7] and approximate[1] values of the drag of a number of cones.* The regions where the curves for $\theta = 12.5°$ and $20°$ depart appreciably from the others correspond to subsonic flow along the cone surface. The curve for $\theta = 12.5°$ in Fig. 1, faired into the slender body curve for small $R\sqrt{M^2-1}/L$, was chosen as the unique curve for all cones as a basis for extending the cone results to open-nose bodies.

The first step of this extension was to choose one of the approximate theories as the preferable one for each value of $R_1\sqrt{M^2-1}/\ell$, where ℓ is the length of a truncated body so that R_1/ℓ is a measure of slope only in conjunction with the area ratio S_o/S_1. For $R_1\sqrt{M^2-1}/\ell = 0.05$, 0.10, 0.15, 0.20, 0.30 the slender body theory was taken, for $R_1\sqrt{M^2-1}/\ell$ = 0.6, 0.8, 1.0 the quasi-cylinder theory was taken, and for $R_1\sqrt{M^2-1}/\ell = 0.4$ a mean of the two was taken. The exact results for cones were then introduced by the following rather arbitrary assumption: that for constant $R_1\sqrt{M^2-1}/\ell$ the percentage difference between 'exact' values and those given by the chosen approximate theory decreases linearly with the area ratio S_o/S_1 as this varies from 0 to 1. Thus if Y is the 'exact' value of $C_D(\ell/R_1)^2$, y is its approximate value, and x is S_o/S_1, then Y is defined by

$$\frac{Y}{y} = 1 + \left[\left(\frac{Y}{y}\right)_{x=0} - 1\right]\left[1 - x\right], \qquad \frac{R_1\sqrt{M^2-1}}{\ell} = \text{constant}.$$

The results of this procedure are shown in Fig. 5.

---

* There is of course no justification for applying the quasi-cylinder theory to pointed bodies but this was done here because at the higher Mach numbers the quasi-cylinder theory gives a less erroneous indication of the variation of drag with Mach number than does the slender body theory. This tendency, which seems to persist for all the bodies considered here, may be partly explained as follows: the quasi-cylinder theory uses the complete solution of the linearised equation, $K_o\left(\sqrt{M^2-1}\ pr\right)$ in the notation of Refs. 1, 2 or 3, although it only satisfies the boundary condition at a mean radius; on the other hand the slender body theory only uses the first two terms of $K_o\left(\sqrt{M^2-1}\ pr\right)$ expanded in ascending powers of its argument.

2.2 Parabolic forebodies

The procedure for obtaining the drag of pointed and open-nose parabolic forebodies was identical with that outlined for conical bodies. The difference in local radius and slope between a circular arc and a parabolic profile with the same overall dimensions is $O[(R_1-R_0)^3/\ell^3]$ and this difference was considered to be negligible to the order of accuracy of the present work. (Strictly only the parabola gives geometrically 'similar' bodies when the thickness ratio is varied). The assumed unique curve for pointed parabolic forebodies (Fig. 2) is based upon the careful characteristics calculations of Rossow[6] for circular arc ogives. The results for open-nose parabolic forebodies, obtained as above, are given in Fig. 6.

2.3 Conical afterbodies

The results for the principal drag of conical afterbodies are based on a number of calculations made with Van Dyke's second-order theory[8]: for these the author is indebted to H. K. Zienkiewicz of the English Electric Co., Ltd. The drag coefficients here have been multiplied by a factor C_{p_1} (exact)/C_{p_1} (second-order), where C_{p_1} is the pressure coefficient immediately behind the initial corner; this factor was always between 1.06 and 1.00 and appeared to improve correlation on the basis of the similarity law. Fig. 3 shows this correlation and the curves assumed unique for each area ratio; the final results are cross-plotted in Fig. 7.

2.4 Parabolic afterbodies

The results for parabolic afterbodies were based on a series of characteristics calculations, performed at the request of the R.A.E. by the Computing Section of the Mathematical Division, NPL, under the supervision of Dr. L. Fox. These results are shown in Fig. 4; the curves assumed unique for each area ratio are those for the body with a basic thickness ratio of 0.1414, extended to higher Mach numbers by extrapolating them parallel to the quasi-cylinder solution. The final results are cross-plotted in Fig 8.

3 Conclusions

The results for afterbodies and pointed forebodies are clearly on firmer ground as solutions of the inviscid flow problem than those for open-nose forebodies because of the assumption made in the latter case about the variation of drag with area ratio. In fact whereas the results for afterbodies and pointed forebodies are presented here with some confidence, those for open-nose forebodies are only intended as a tentative guide to enable designers to make rapid estimates of drag which will not be altogether unreasonable.

On the other hand the effect of boundary layer upon the pressure distribution and wave drag is in general appreciable only for afterbodies: this effect is usually favourable.

It has been seen that the similarity law 'collapses' exact results remarkably well; it should be noted, however, that when a curve representing some typical thickness ratio is assumed to be unique, it always overestimates slightly the drag of thicker bodies and underestimates slightly the drag of more slender ones. Allowance for this effect, if desired, can be made by referring to Figs. 1 to 4.

NOTATION

C_D	wave drag coefficient based on maximum cross-sectional area
ℓ	length of a truncated forebody or afterbody
L	length of a pointed forebody or afterbody
M	free stream Mach number
R	radius
S	cross-section area
$(\ )_0$	station of minimum cross-sectional area
$(\ )_1$	station of maximum cross-sectional area

REFERENCES

No.	Author	Title, etc.
1	L.E. Fraenkel	The theoretical wave drag of some bodies of revolution. ARC R&M 2842, (RAE Report Aero 2420, 1951), ARC No. 14,334.
2	G.N. Ward	The approximate external and internal flow past a quasi-cylindrical tube moving at supersonic speeds. Quart. Jour. Mech. and Appl. Maths., Vol. 1 Part 2, June, 1948.
3	M.J. Lighthill	Supersonic flow past slender bodies of revolution the slope of whose meridian section is discontinuous. Quart. Jour. Mech. and Appl. Maths. Vol. 1 Part 1, March, 1948.
4	H.S. Tsien	Similarity laws of hypersonic flows. Jour. Maths. and Phys., Vol. 25 No. 3, October, 1946.
5	W.D. Hayes	On hypersonic similitude. Quart. Appl. Maths., Vol. 5, No. 1, April, 1947.

REFERENCES (Contd)

No.	Author	Title, etc
6	V.J. Rossow	Applicability of the hypersonic similarity rule to pressure distributions which include the effects of rotation for bodies of revolution at zero angle of attack. NACA Tech. Note 2399, 1951.
7	Z. Kopal	Tables of supersonic flow around cones. M.I.T. Tech. Report No.1, Cambridge, Mass., 1947.
8	M.D. Van Dyke	A study of second-order supersonic flow theory. NACA Tech. Note 2200, 1951. ARC 13,981

Wt.2078.CP136.K3. Printed in Great Britain.

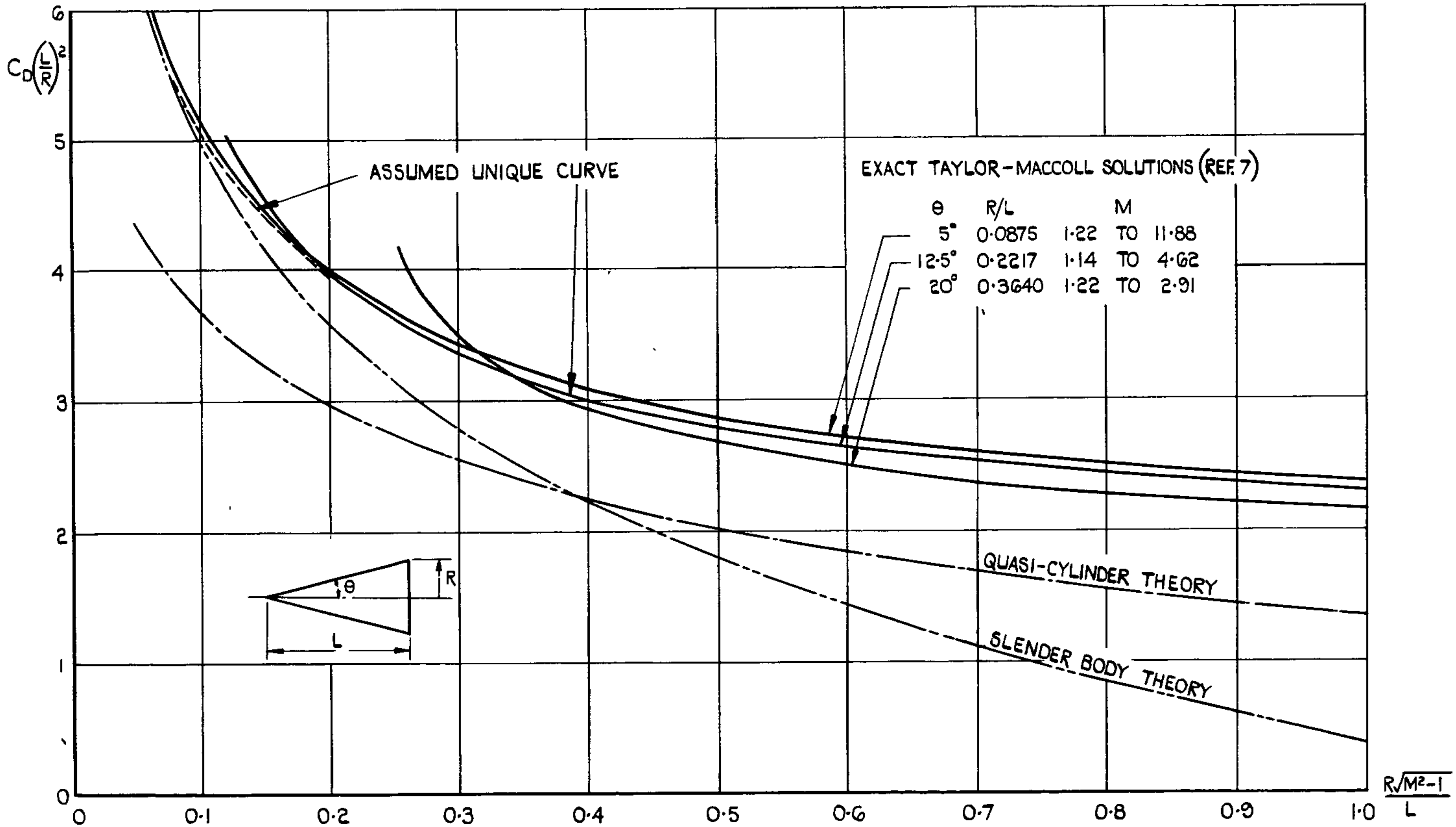

FIG. 1 EXACT AND APPROXIMATE RESULTS FOR CONES

FIG. 1

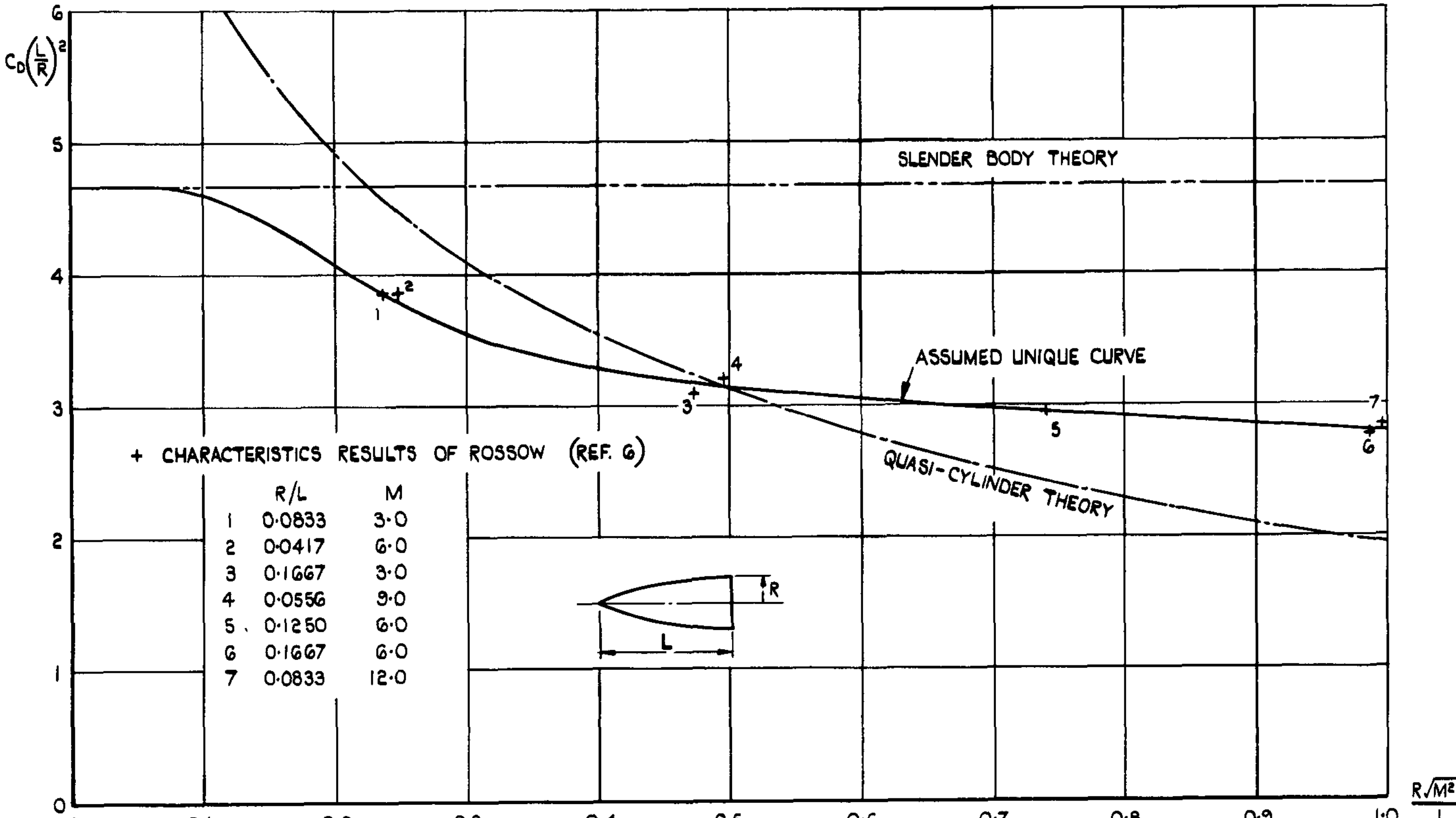

FIG.2 EXACT AND APPROXIMATE RESULTS FOR POINTED PARABOLIC (OR OGIVAL) FOREBODIES.

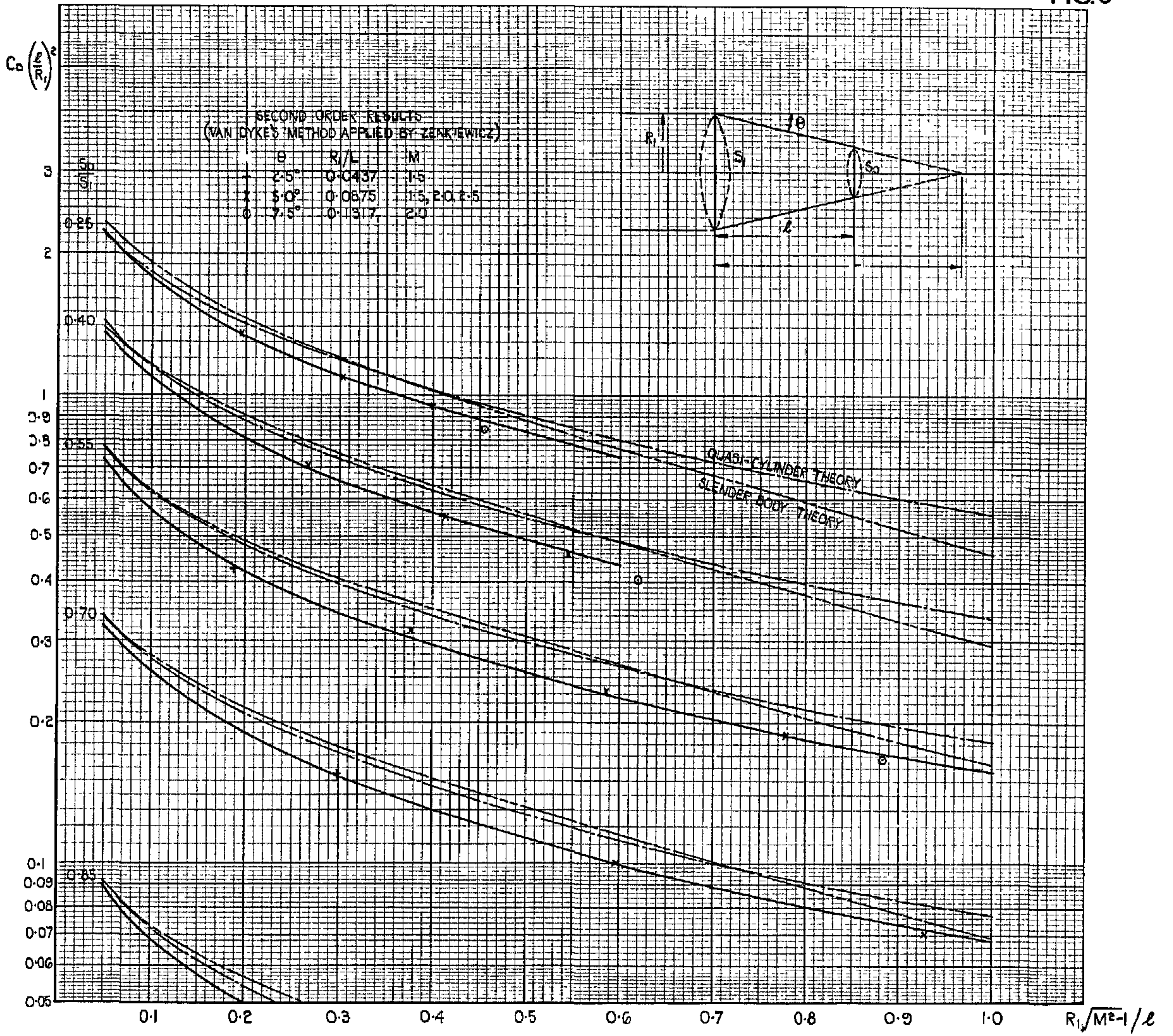

FIG. 3 SECOND-ORDER AND APPROXIMATE RESULTS FOR CONICAL AFTERBODIES

FIG. 4

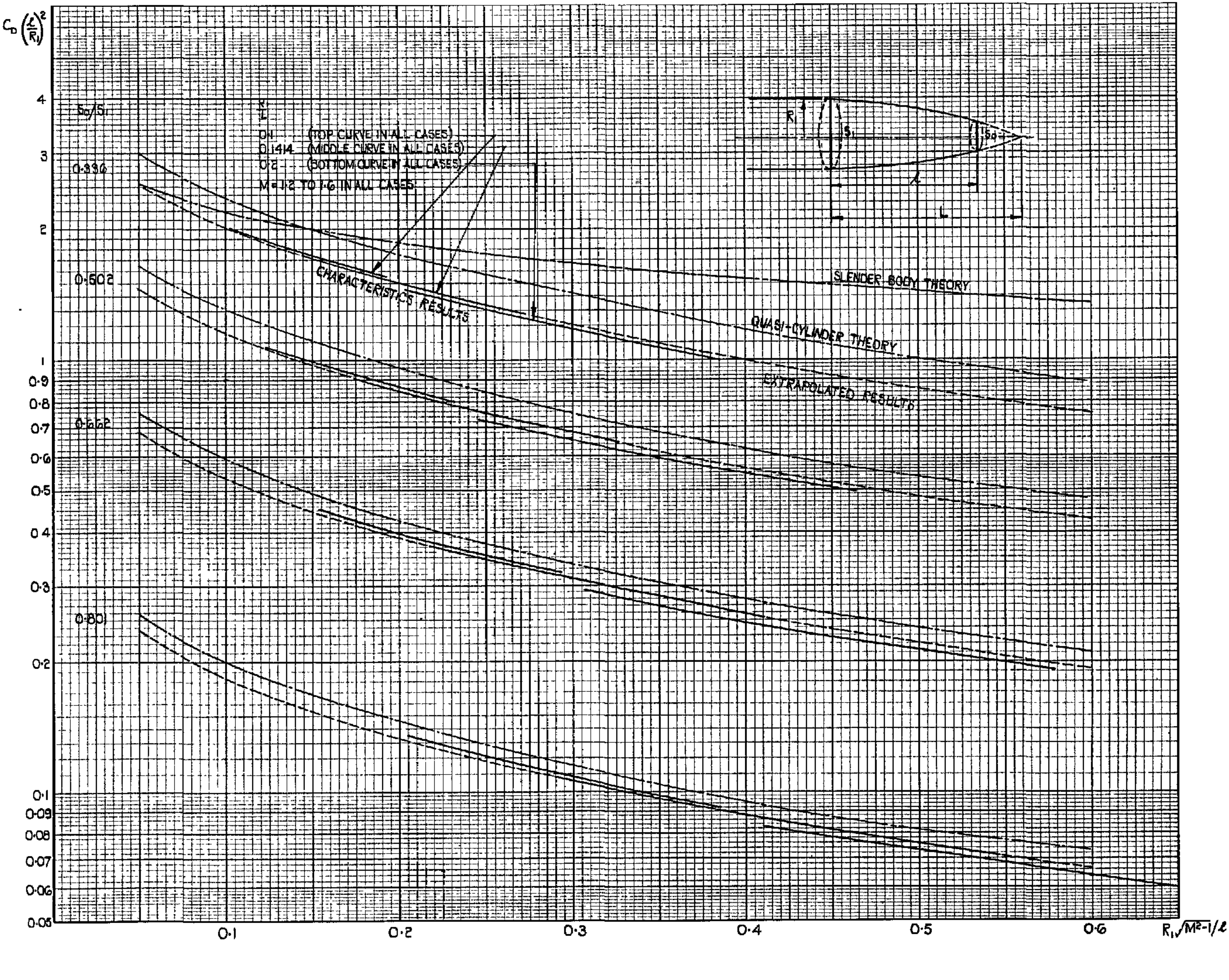

FIG. 4 EXACT AND APPROXIMATE RESULTS FOR PARABOLIC AFTERBODIES.

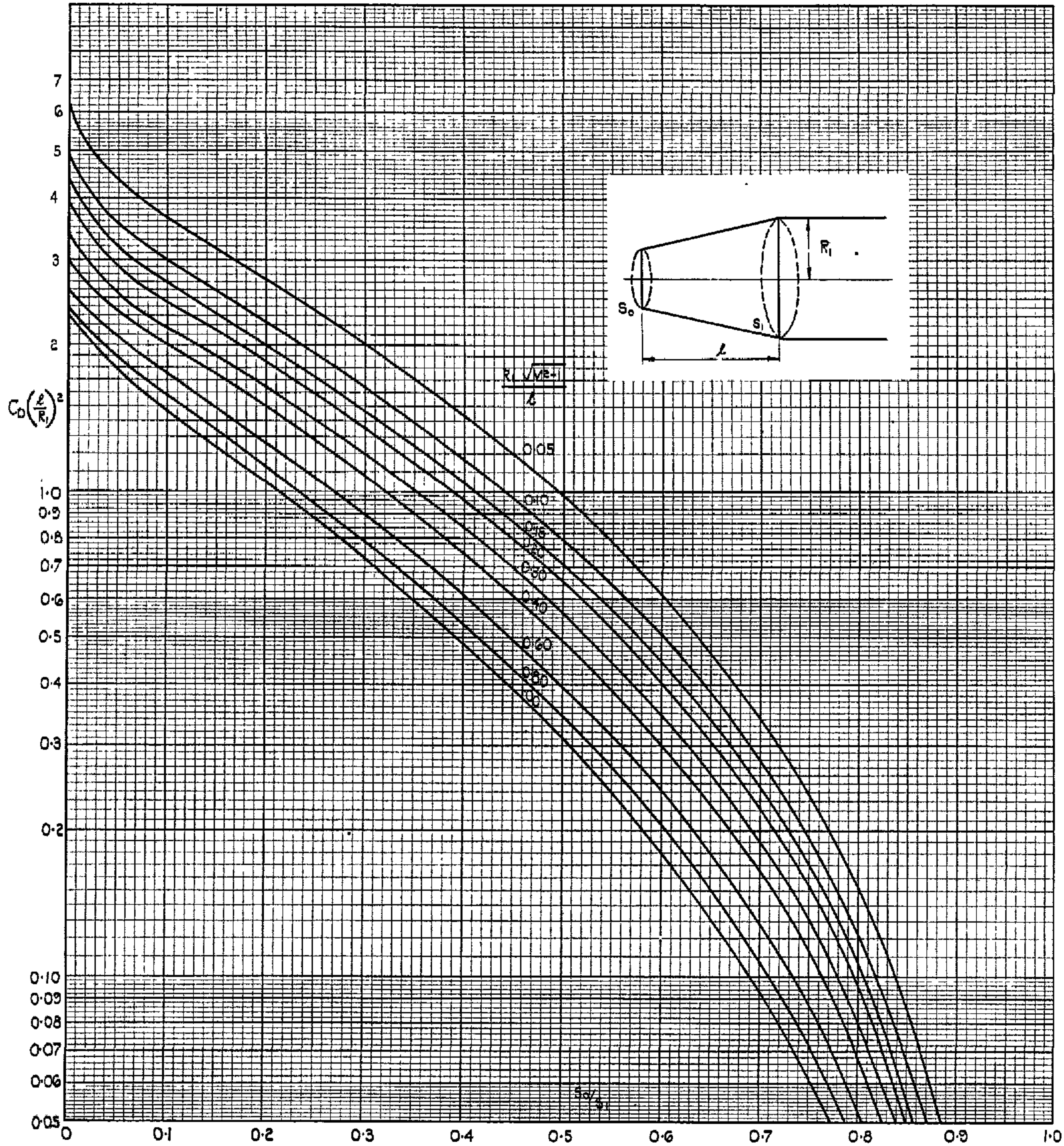

FIG. 5 SUPERSONIC WAVE DRAG OF CONICAL FOREBODIES.

FIG. 6

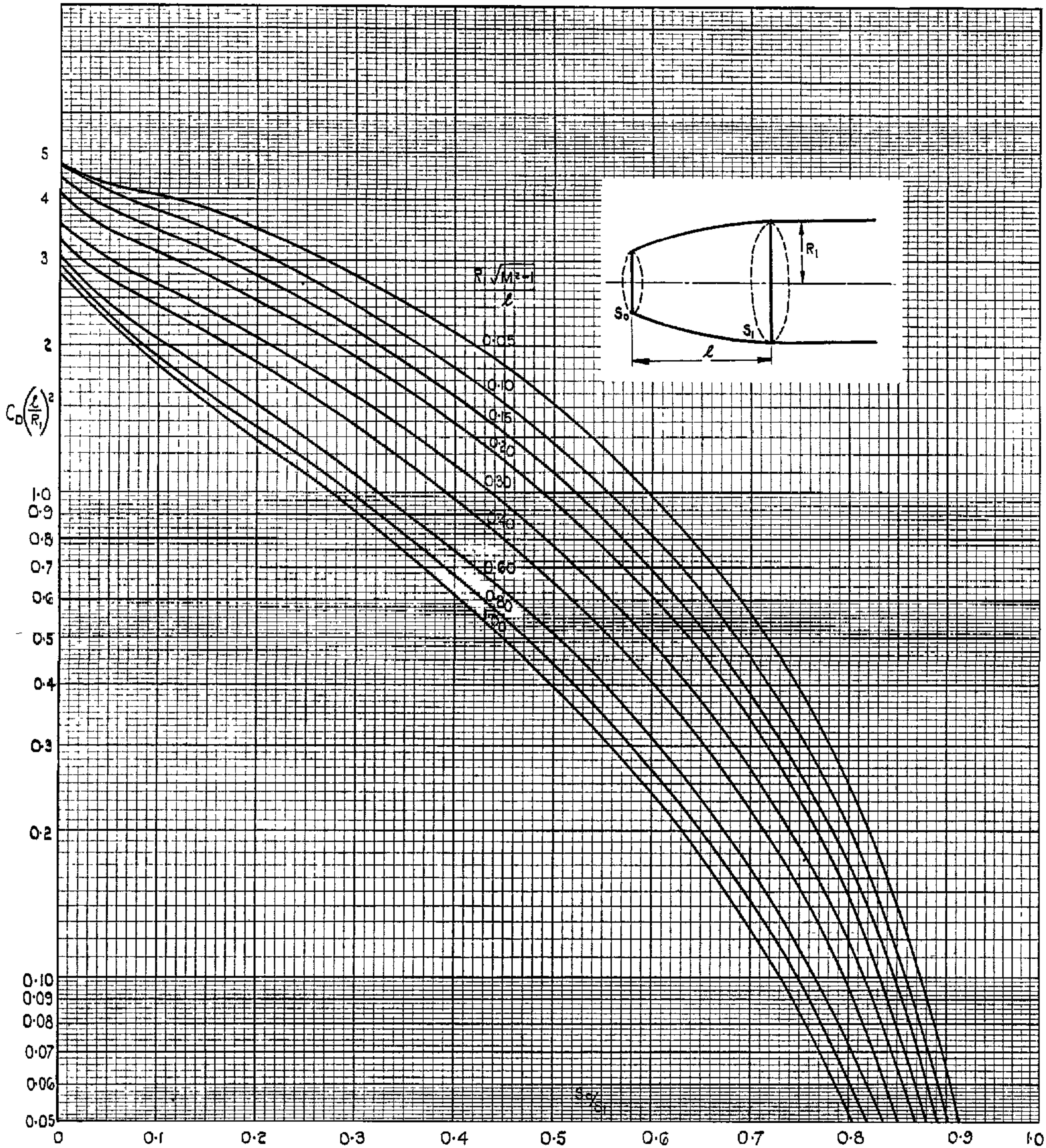

FIG.6 SUPERSONIC WAVE DRAG OF PARABOLIC FOREBODIES.

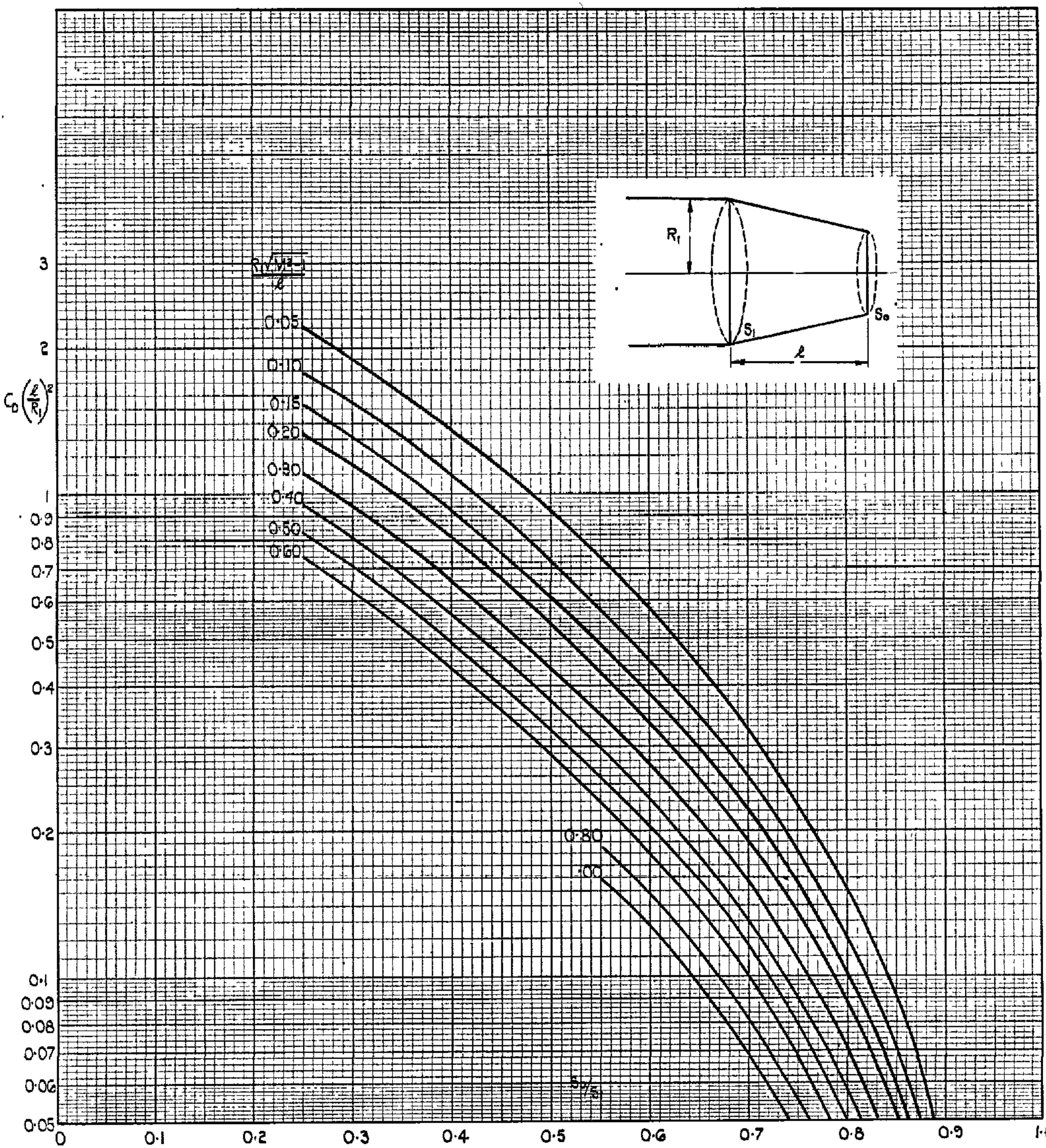

FIG. 7 SUPERSONIC WAVE DRAG OF CONICAL AFTERBODIES.

FIG.8

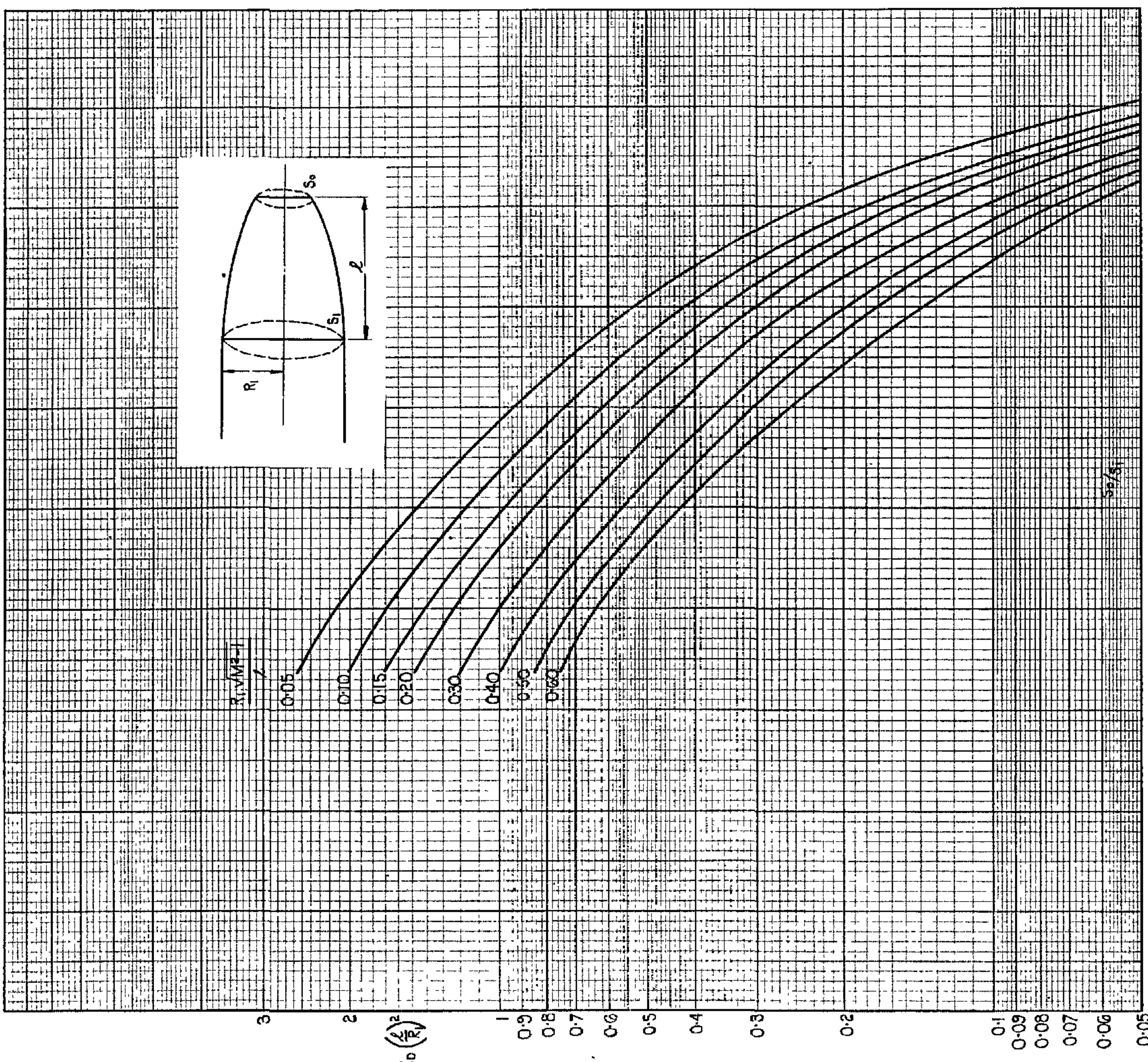

FIG.8 SUPERSONIC WAVE DRAG OF PARABOLIC AFTERBODIES.

C.P. No. 136
(15,685)
A.R.C. Technical Report

PUBLISHED BY HER MAJESTY'S STATIONERY OFFICE

To be purchased from
York House, Kingsway, LONDON, W C 2. 423 Oxford Street, LONDON, W.1
P.O. Box 569, LONDON, S E 1
13a Castle Street, EDINBURGH, 2 | 1 St. Andrew's Crescent, CARDIFF
39 King Street, MANCHESTER, 2 | Tower Lane, BRISTOL, 1
2 Edmund Street, BIRMINGHAM, 3 | 80 Chichester Street, BELFAST
or from any Bookseller

1953

Price 3s. 0d. net
PRINTED IN GREAT BRITAIN

S.O. Code No. 23-9007-36